

## White light generation tuned by dual hybridization of nanocrystals and conjugated polymers

Hilmi Volkan Demir<sup>1,2,3,6</sup>, Sedat Nizamoglu<sup>1,2</sup>, Tuncay Ozel<sup>1,2</sup>,  
Evren Mutlugun<sup>1,2</sup>, Ilkem Ozge Huyal<sup>1,4</sup>, Emre Sari<sup>1,3</sup>,  
Elisabeth Holder<sup>5</sup> and Nan Tian<sup>5</sup>

<sup>1</sup> Devices and Sensors Group and Nanotechnology Research Center,  
Bilkent University, Ankara 06800, Turkey

<sup>2</sup> Department of Physics, Bilkent University, Ankara 06800, Turkey

<sup>3</sup> Department of Electrical and Electronics Engineering, Bilkent University,  
Ankara 06800, Turkey

<sup>4</sup> Department of Chemistry, Bilkent University, Ankara 06800, Turkey

<sup>5</sup> Functional Polymers Group and Institute of Polymer Technology,  
University of Wuppertal, Gaußstrasse 20, D-42097 Wuppertal, Germany  
E-mail: [volkan@bilkent.edu.tr](mailto:volkan@bilkent.edu.tr) and [holder@uni-wuppertal.de](mailto:holder@uni-wuppertal.de)

*New Journal of Physics* **9** (2007) 362

Received 29 May 2007

Published 5 October 2007

Online at <http://www.njp.org/>

doi:10.1088/1367-2630/9/10/362

**Abstract.** Dual hybridization of highly fluorescent conjugated polymers and highly luminescent nanocrystals (NCs) is developed and demonstrated in multiple combinations for controlled white light generation with high color rendering index (CRI) ( $> 80$ ) for the first time. The generated white light is tuned using layer-by-layer assembly of CdSe/ZnS core-shell NCs closely packed on polyfluorene, hybridized on near-UV emitting nitride-based light emitting diodes (LEDs). The design, synthesis, growth, fabrication and characterization of these hybrid inorganic–organic white LEDs are presented. The following experimental realizations are reported: (i) layer-by-layer hybridization of yellow NCs ( $\lambda_{\text{PL}} = 580$  nm) and blue polyfluorene ( $\lambda_{\text{PL}} = 439$  nm) with tristimulus coordinates of  $(x, y) = (0.31, 0.27)$ , correlated color temperature of  $T_c = 6962$  K and CRI of  $R_a = 53.4$ ; (ii) layer-by-layer assembly of yellow and green NCs ( $\lambda_{\text{PL}} = 580$  and  $540$  nm) and blue polyfluorene ( $\lambda_{\text{PL}} = 439$  nm) with  $(x, y) = (0.23, 0.30)$ ,  $T_c = 14395$  K and  $R_a = 65.7$ ; and (iii) layer-by-layer

<sup>6</sup> Author to whom any correspondence should be addressed.

deposition of yellow, green and red NCs ( $\lambda_{\text{PL}} = 580, 540$  and  $620$  nm) and blue polyfluorene ( $\lambda_{\text{PL}} = 439$  nm) with  $(x, y) = (0.38, 0.39)$ ,  $T_c = 4052$  K and  $R_a = 83.0$ . The CRI is demonstrated to be well controlled and significantly improved by increasing multi-chromaticity of the NC and polymer emitters.

Recently solid-state lighting using white light emitting diodes (WLEDs) has attracted worldwide attention because of their important benefits including energy saving, safety, reliability and maintenance [1]. In the world, it is estimated that 20% of the global electricity production is currently consumed for lighting and that solid-state lighting offers potentially 50% reduction globally in the electricity consumption for illumination [2]. Furthermore, today approximately one-third of the world population (about two billion people) has no access to electricity and relies on fuel-based lighting for home illumination. However, fuel-based lighting provides an unhealthy and costly means of illumination with low light quality (i.e. with low color rendering index (CRI)). To supply safe, healthy and affordable white light around the globe, the Light Up The World Foundation strongly advocates the use of WLEDs [3]. To this end, such a worldwide strong demand for the development of high quality WLEDs around the globe motivates the investigation of white light generation with high CRI.

Today incandescent and fluorescent light sources are widely used. Among these, compact fluorescent lamps (energy saving light bulbs) offer significant reduction in energy loss (30%) compared to the incandescent lamps (90%) but very few dimmable products of such lamps are currently available [4]. As an alternative, WLEDs that are conveniently dimmable while independently keeping their operating points are increasingly being used for architectural lighting [5]. In the future it is expected that LED-based white light sources will completely replace traditional incandescent and fluorescent lamps and, even within the next five years, it is predicted that WLEDs will be employed for all external lighting functions on vehicles in the automotive industry [6]. To date different approaches of such solid state lighting including multi-chip WLEDs, monolithic WLEDs and color conversion WLEDs (commonly using phosphors) have been investigated [7]–[9]. Among these, the WLED based on phosphor coating was first commercialized in 1996 [7]. Such color-conversion LEDs utilize electroluminescence (EL) of the LED platform and photoluminescence (PL) of luminescent phosphor film integrated on this platform. However, although phosphor is good for providing broadband photoemission, there are problems associated with its usage. These problems arise due to the difficulties in controlling granule size and in mixing and depositing uniform films of phosphors, which lead to undesired visible color variations as one of the most fundamental disadvantages [10]. Also, the CRI of such phosphor-based color conversion can be undesirably low for high quality lighting. For example, yellow phosphor-based WLEDs typically exhibit color-rendering indices of about 70, whereas the future solid-state lighting requirements dictate a CRI above 80 [11]. Moreover, although the emission of phosphor can be modified by substituting different chemicals (e.g. Gd for Y, Ga for Al) and red-emitting phosphor can be used for color temperature adjustment, their broad emission spectrum makes it relatively more difficult to fully tune the properties of the generated white light (e.g. the tristimulus coordinates and color temperature), as is required to achieve optimal lighting conditions specific to particular applications (e.g., in museums, shop windows, etc) [7].

As a possible remedy to overcome these disadvantages, hybrid organic–inorganic LEDs could reveal an effective form of lighting for the desired high quality. With their promising

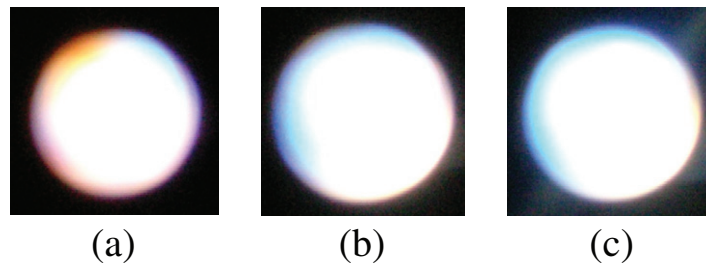
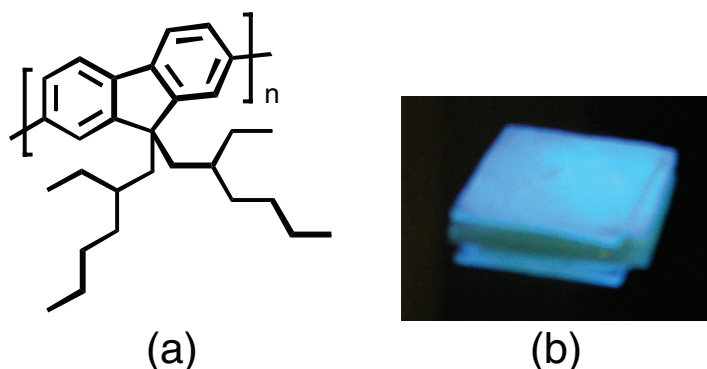


**Figure 1.** Images of white light emission from hybrid NC-conjugated polymer-based WLEDs: (a) yellow NCs ( $\lambda_{\text{PL}} = 580$  nm) and blue polyfluorene ( $\lambda_{\text{PL}} = 439$  nm), (b) yellow and green NCs ( $\lambda_{\text{PL}} = 580$  and 540 nm) and blue polyfluorene ( $\lambda_{\text{PL}} = 439$  nm) and (c) yellow, green and red NCs ( $\lambda_{\text{PL}} = 580$ , 540 and 620 nm) and blue polyfluorene ( $\lambda_{\text{PL}} = 439$  nm), all hybridized on n-UV LEDs ( $\lambda_{\text{EL}} = 383$  nm).

optical properties, polymers and nanocrystals (NCs) are potential candidates for future high-quality lighting technology. In this paper, the dual hybridization of highly fluorescent conjugated polymers and highly luminescent NCs is introduced in multiple combinations for controlled white light generation with high CRI for the first time (shown in figure 1). Here, the white light generation is tuned using layer-by-layer assembly of closely packed CdSe/ZnS core-shell NCs and polyfluorene conjugated polymer hybridized on near-UV emitting nitride-based LEDs. The design, synthesis, growth, fabrication and characterization of these hybrid inorganic–organic WLEDs are described.

White light generation utilizing different polymers has previously been investigated [12]–[22]. Among various polymer types, specifically conjugated polymers are promising candidates in lighting applications. They have very strong absorption both in n-UV and blue on the order of  $10^5 \text{ cm}^{-1}$  with very high quantum efficiency [10]. Additionally, polymers can be deposited easily with common techniques such as spin coating and noticeably they are almost free from concentration quenching effects. Similarly, NCs have also recently been used for color conversion in white light generation. They also show very promising properties including narrow emission spectra widely tunable across the visible spectral range, small overlap between their emission and absorption spectra, and the ability to easily and uniformly deposit their films with common techniques such as evaporation, spin casting and dip coating. NC-based WLEDs have been achieved with significant progress only in recent years. White light generation using CdSe/ZnS core-shell NCs of single, dual, trio and quadruple combinations hybridized with blue InGaN/GaN LEDs have been shown in our previous work [23, 24]. Also, a blue/green two-wavelength InGaN/GaN LED coated with a single type of red NC and a blue InGaN/GaN LED with a single type of yellow NC and a dual type of red and green NCs have also been reported [25, 26]. Furthermore, a WLED has been fabricated by coating a blended mixture of CdSeS NCs with polymethylmethacrylate on a commercial UV-LED [27] and also by layer-by-layer assembly of CdSe/ZnS NCs on a near-UV LED [28]. Additionally, a large set of 26 different samples have been implemented to study the NC hybridization on nitride-based LEDs [29].

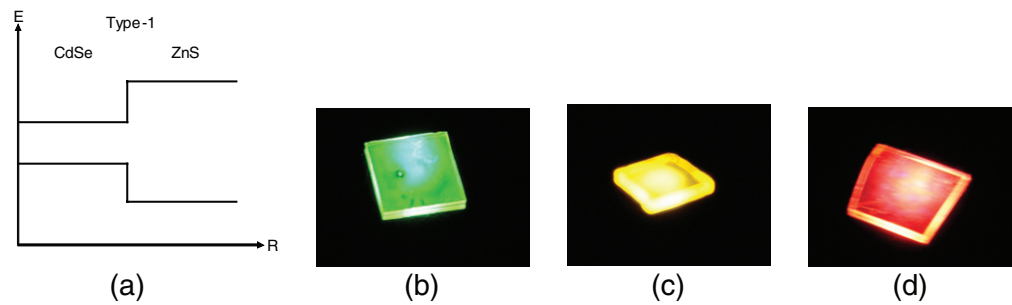
In this paper, unlike in previous research work, the combined use of conjugated polymers and NCs for white light generation on the same n-UV LED platform is shown. The white light



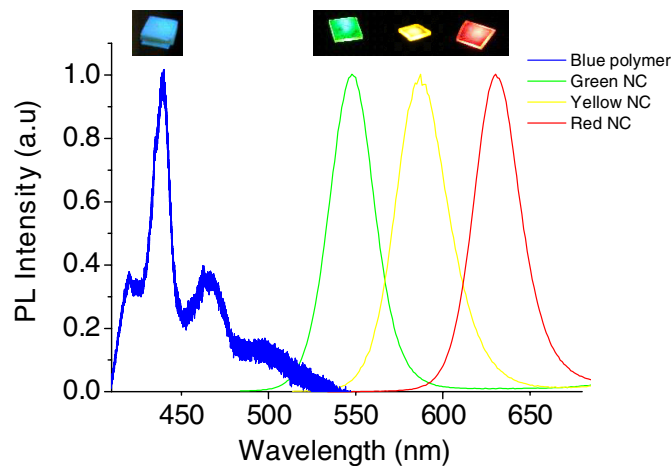
**Figure 2.** (a) Chemical structure of 9,9-*bis*(2-ethylhexyl)polyfluorene that is hybridized on the n-UV-LEDs and (b) photograph of its PL in blue.

generation by different combinations of polyfluorene and NCs affording high color rendering indices is demonstrated; the tunability of the generated white light is studied. In this work, the combinations incorporated on our n-UV LEDs include (i) yellow NCs ( $\lambda_{\text{PL}} = 580$  nm) and blue polyfluorene ( $\lambda_{\text{PL}} = 439$  nm) with tristimulus coordinates of  $(x, y) = (0.31, 0.27)$ , a correlated color temperature of  $T_c = 6962$  K and a CRI of  $R_a = 53.4$  shown in figure 1(a); (ii) yellow and green NCs ( $\lambda_{\text{PL}} = 580$  and 540 nm) and blue polyfluorene ( $\lambda_{\text{PL}} = 439$  nm) with  $(x, y) = (0.23, 0.30)$ ,  $T_c = 14395$  K and  $R_a = 65.7$  shown in figure 1(b); and (iii) yellow, green and red NCs ( $\lambda_{\text{PL}} = 580, 540$  and 620 nm) and blue polyfluorene ( $\lambda_{\text{PL}} = 439$  nm) with  $(x, y) = (0.38, 0.39)$ ,  $T_c = 4052$  K and  $R_a = 83.0$  shown in figure 1(c). Here, along with NCs emitting in red, yellow and green, the polyfluorene serves an important function of efficient emission in blue, for it is much more difficult to obtain high efficiency emission with NCs at the shorter wavelengths (for example, in the blue range). With such dual use of polyfluorene and NCs, the CRI is well controlled and significantly improved by increasing the multi-chromaticity of the NC and polymer emitters. In so doing, high CRI ( $> 80$ ) exceeding the requirements of the future solid state lighting applications is achieved.

Figure 2(a) shows the chemical structure of the hybridized 9,9-*bis*(2-ethylhexyl)-polyfluorene, which is obtained following a synthetic protocol according to Yamamoto [19], [30]–[32]. 2,7-Dibromo-9,9-*bis*(2-ethylhexyl)fluorene (0.855 mmol, 500 mg), Ni(COD)<sub>2</sub> (1.881 mmol, 1.034 g) and 2,2'-bipyridyl (1.881 mmol, 293.7 mg) are mixed together with 25 ml of degassed THF and COD (1.881 mmol, 166  $\mu$ ml) under argon atmosphere in a 50 ml Schlenk tube. The mixture is stirred at 80 °C for three days in the dark. The reaction mixture is suspended into CHCl<sub>3</sub> (50 ml), washed with H<sub>2</sub>O, saturated NaEDTA solution ( $3 \times 100$  ml) and saturated NaHCO<sub>3</sub> solution ( $3 \times 100$  ml), dried over anhydrous MgSO<sub>4</sub>. After removing the solvent under reduced pressure, the polymer is precipitated into MeOH and purified by washing with refluxing EtOAc in a Soxhlet apparatus for one day. The polymer is dried under vacuum at 60 °C to afford 290 mg (58%) of a yellow solid. The polymer is obtained with a high molecular weight  $M_n = 42\,000$  g mol<sup>-1</sup>,  $M_w = 79\,000$  g mol<sup>-1</sup>, and a reasonable polydispersity index (PDI) = 1.88. The thermal gravimetric analysis (TGA) shows a high thermal stability up to 432 °C, which is of importance for LED applications. The absorption maximum in CHCl<sub>3</sub> solution is  $\lambda_{\text{max,abs}} = 382$  nm, while its emission maximum is  $\lambda_{\text{PL}} = 414$  nm, as shown while photoemitting in blue in the form of a thin film in figure 2(b). In the hybrid LED architectures



**Figure 3.** (a) type-1 band alignment of CdSe/ZnS core-shell NC and PL photographs of (b) the green NC film, (c) the yellow NC film and (d) the red NC film.

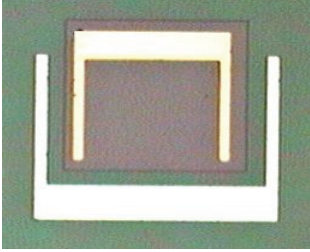


**Figure 4.** PL spectra of the blue emitting conjugated polymer polyfluorene, and green, yellow and red emitting CdSe/ZnS NCs.

that incorporate conjugated polymers as the color converting film, the polymer is typically found to limit the device lifetime. With properly encapsulating polymer, such hybrid LEDs are shown to operate over 5000 h [33].

In addition to the polyfluorene conjugated polymer, three types of NCs are utilized as color-selectable emitters with tunable PL in the visible spectral range. These NCs are made of CdSe/ZnS core-shell structures with type-1 band alignment as sketched in figure 3(a). Their emission colors are green, yellow and red (shown in figures 3(b)–(d)), tuned using the quantum size effect across the visible with their corresponding PL peaks at 540, 580 and 620 nm, respectively. The PL of the polymer and NC emitters in thin films are shown altogether in figure 4. These NCs available from Evident have high PL quantum yields ranging between 30 and 50%. Such core-shell NCs have been shown to yield even higher efficiencies up to 66% [34]. These NCs have crystal diameters of 2.4, 3.2 and 5.2 nm and exhibit a size distribution of  $\pm 5\%$ . Their respective molecular weights are 14, 38 and  $180 \mu\text{g nmol}^{-1}$ . Such types of NCs have been used in our previous work for white light sources integrated on nitride LEDs [23, 29] and NC-based UV scintillators integrated on Si detectors [35]. In this work, high concentration NC solutions are prepared and NC films are evaporated for optimal film formation. Here, the



**Table 1.** Micrograph of the fabricated n-UV LED and its epitaxial structure.


Layer	Thickness (nm)
p-GaN	120
p-AlGaN	50
p-GaN	4
InGaN (well) $\times$ 5	2–3
GaN (barrier) $\times$ 5	2–3
n-GaN	690
GaN (buffer)	200
GaN (nucleation)	14
Sapphire	Substrate

hybrid device parameters including the type and film thickness of closely packed NC emitters, the concentration and film thickness of polymer emitters, and the order of NC and polymer films are controlled to adjust optical properties of the generated white light. These parameters affect the color conversion rate and thus the relative optical power of NC and polymer PL peaks contributing to the spectrum. By using different numbers of NC–polymer combinations, the intervals of the spectrum to contribute to the white light generation are set. By changing the order of NC and polymer films, the level of reabsorption of the photons emitted by the previous layers is adjusted. By increasing the number of combinations, multi-chromatic sources are achieved to generate white light with high color rendering indices. Such an ability to control these hybrid device parameters enables tuning of the optical properties of the generated white light as desired.

All hybrid devices are implemented on InGaN/GaN-based LED pump sources with a peak wavelength of 383 nm in the near UV. Table 1 shows the design of the fabricated LEDs along with the thickness of each epitaxial layer and a micrograph of one of these fabricated devices. The InGaN/GaN quantum structures are grown on a *c*-plane sapphire using metal organic chemical vapor deposition (MOCVD) system (Aixtron RF200/4 RF-S). At first a 14 nm thick GaN nucleation layer and a 200 nm thick GaN buffer layer are deposited. Here, the buffer layer plays an important role in achieving higher crystal quality. Subsequently, a 690 nm thick Si-doped n-type GaN epitaxial layer is grown and, on top of it, 2–3 nm thick InGaN wells and GaN barriers are grown at a growth temperature of 720 °C. Finally, a 4 nm thick Mg-doped p-type GaN layer, a 50 nm thick Mg-doped p-type AlGaN layer, and a 120 nm thick Mg-doped GaN layer are grown as the contact layers. Afterwards, Mg dopants are activated at 750 °C for 15 min. The epitaxial growth is monitored at all times by *in situ* optical reflectance, and the growth temperature is controlled using two infrared pyrometers. Further, for the definition of device mesas and electrical contacts, the standard semiconductor processing procedures follow photolithography, thermal evaporation (metallization), reactive ion etching (RIE) and rapid thermal annealing, as also included in our previous work [36]–[39]. To lay down n-contacts, the wafer is etched with RIE down to reach the n-contact layer, and a 10 nm thick Ti film with a 200 nm over-layer of Al is deposited as the metal contacts. The metallization is then carried out by subsequent rapid thermal annealing at 600 °C for 1 min under nitrogen to prevent oxidization. For the p-contacts, metal deposition of a 15 nm thick Ni film with a 100 nm over-layer of Au followed by rapid thermal annealing at 700 °C for 30 s is completed.

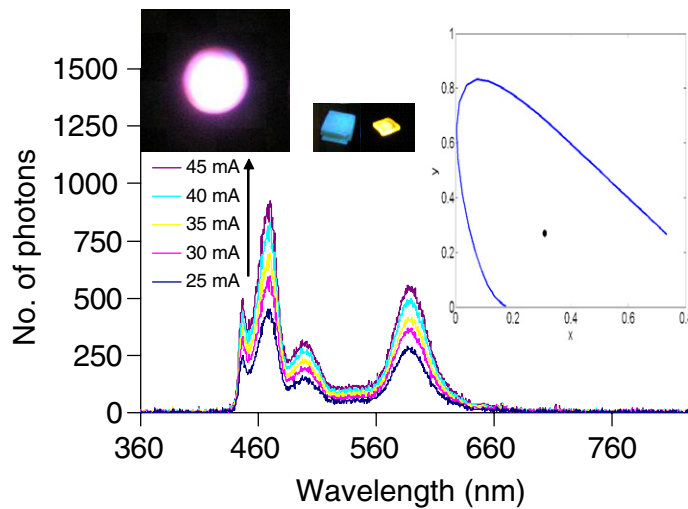


**Figure 5.** EL spectra of yellow CdSe/ZnS core-shell NCs ( $\lambda_{\text{PL}} = 580$  nm) and blue polyfluorene conjugated polymer ( $\lambda_{\text{PL}} = 439$  nm) deposited layer-by-layer on an InGaN/GaN n-UV LED ( $\lambda_{\text{EL}} = 383$  nm) at different levels of current injection (at room temperature). Pictures of the generated white light, blue emission of the polymer and yellow emission of the NCs are shown. The location of the corresponding operating point on the  $(x, y)$  chromaticity coordinates is also displayed.

To obtain white light, our InGaN/GaN n-UV LED ( $\lambda_{\text{EL}} = 383$  nm) is first integrated with blue emitting polyfluorene polymers ( $\lambda_{\text{PL}} = 439$  nm) and single type yellow CdSe/ZnS core-shell NCs ( $\lambda_{\text{PL}} = 580$  nm) on the top. The hybridization parameters are carefully designed to satisfy the white light condition with the highest possible CRI, considering the optical properties of the polyfluorene, NC and LED. For that, a 135 nm thick layer of closely packed yellow NCs and a 1.06  $\mu\text{m}$  thick layer of 3 mg ml<sup>-1</sup> blue polymer are hybridized on to the LED. The resulting hybrid LED is characterized on a probe station with dc probes placed on the LED to electrically drive it by current power supply (HP4142B Modular dc Source/Monitor), while collecting the emitted light through an optical system to couple into a multimode fiber connected to an optical spectrum analyzer setup (Ocean Optics PC2000 with an optical resolution of 0.5 nm). The EL spectra are obtained at different levels of current injection to the LED at room temperature as shown in figure 5. These emission spectra experimentally yield tristimulus coordinates of  $x = 0.31$  and  $y = 0.27$ , a correlated color temperature of  $T_c = 6962$  K and a CRI of  $R_a = 53.4$ . This operating point falls into the white region in the 1931 CIE chromaticity diagram depicted in figure 5. In our previous work, for such a dichromatic source where only yellow NCs ( $\lambda_{\text{PL}} = 580$  nm) were hybridized on a 440 nm blue InGaN/GaN LED, a CRI of at most 14.6 was acquired [23, 24]. Here instead of blue LEDs, using blue polyfluorene, whose emission spectrum is broader, a higher CRI is achieved. However, given the requirements of future lighting, this CRI is yet not sufficient, which motivates further hybridization of other NC emitters on the hybrid device.

For the second set, instead of using a single NC film, two types of green and yellow CdSe/ZnS core-shell NCs ( $\lambda_{\text{PL}} = 540$  and 580 nm) in combination with the blue emitting polyfluorene ( $\lambda_{\text{PL}} = 439$  nm) are hybridized on our InGaN/GaN n-UV LED ( $\lambda_{\text{EL}} = 383$  nm).

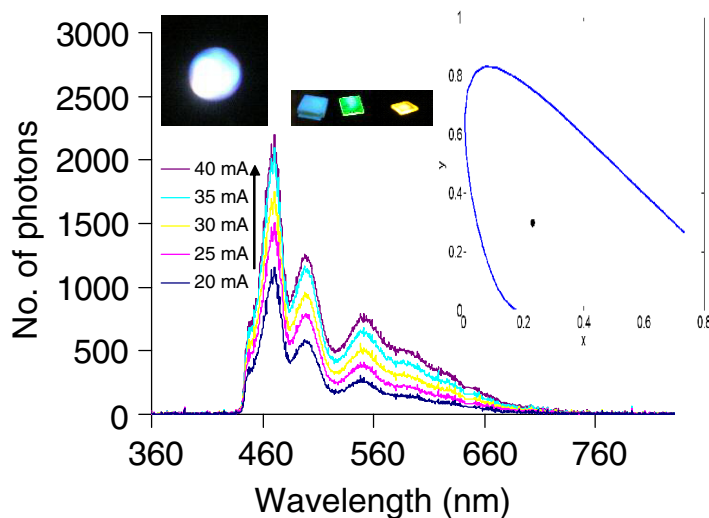


**Figure 6.** EL spectra of blue polyfluorene ( $\lambda_{\text{PL}} = 439$  nm) and green and yellow CdSe/ZnS core-shell NCs ( $\lambda_{\text{PL}} = 540$  and  $580$  nm) layer-by-layer hybridized on an InGaN/GaN n-UV LED ( $\lambda_{\text{EL}} = 383$  nm) at different levels of current injection (at room temperature) along with a picture of the white light generated collectively by the blue polymer and green and yellow NC emissions; and the location of the corresponding operating point on the  $(x, y)$  coordinates.

For this combination, the right hybridization parameters are again carefully selected to increase the CRI while satisfying the white light condition. For this, a  $1.06 \mu\text{m}$  thick film of  $3 \text{ mg ml}^{-1}$  blue polymer followed by a  $400 \text{ nm}$  thick film of closely packed green NCs and topped by a  $70 \text{ nm}$  thick film of closely packed yellow NCs are used. The EL spectra of the resulting hybrid device obtained at different levels of current injection at room temperature are shown in figure 6. This implementation experimentally leads to tristimulus coordinates of  $x = 0.23$  and  $y = 0.30$ , a correlated color temperature of  $T_c = 14\,395 \text{ K}$  and a CRI of  $R_a = 65.7$ , which again mathematically corresponds to the white region of the CIE chromaticity diagram as desired. Here with the right design, a significant improvement in the CRI is achieved as the chromaticity is increased from a dichromatic source to a trichromatic source by the addition of green NCs.

For the third set, rather than using a dual NC combination, three types of NCs (yellow, green, and red at  $\lambda_{\text{PL}} = 580, 540$  and  $620 \text{ nm}$ , respectively) are integrated with blue polyfluorene ( $\lambda_{\text{PL}} = 439 \text{ nm}$ ) on our InGaN/GaN n-UV LED ( $\lambda_{\text{EL}} = 383 \text{ nm}$ ). Again, the hybrid device is carefully designed for increased white light quality. The color properties of the resulting hybrid LED are monitored step by step after hybridization of each emitter layer. Firstly, a  $1.03 \mu\text{m}$  thick layer of  $3 \text{ mg ml}^{-1}$  blue polymer is hybridized on top of the n-UV LED (named CRI test sample 1 here). In this case, the resulting EL corresponds to tristimulus coordinates of  $x = 0.18$  and  $y = 0.21$ , a correlated color temperature of  $T_c = 34\,463 \text{ K}$  and a CRI of  $R_a = 49.5$ . After further integrating an approximately  $400 \text{ nm}$  thick film of closely packed green NCs on top of the polymer, the optical properties are shifted to  $x = 0.32$  and  $y = 0.37$  to fall into the white region with  $R_a = 66.0$  and  $T_c = 5896 \text{ K}$  (named CRI test sample 2). With this additional emitter layer, the CRI increases by approximately 16 units and the color temperature decreases by  $28\,567 \text{ K}$



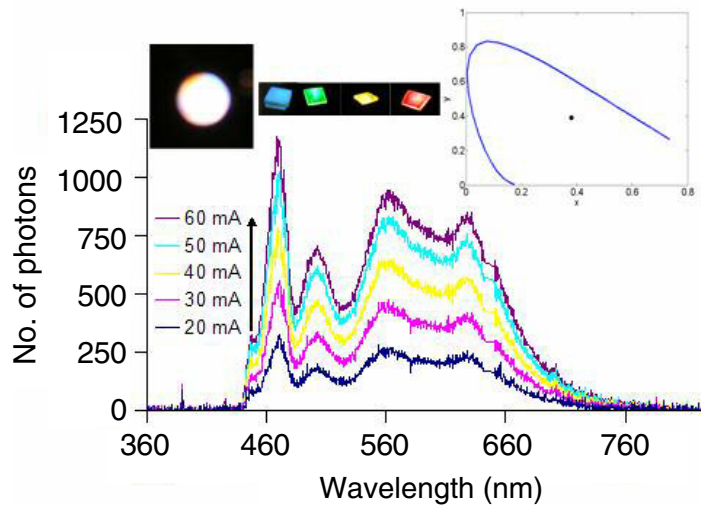


**Figure 7.** EL spectra of blue polyfluorene ( $\lambda_{\text{PL}} = 439$  nm) and yellow, green and red CdSe/ZnS core-shell NCs ( $\lambda_{\text{PL}} = 580, 540$  and  $620$  nm) layer-by-layer hybridized on a InGaN/GaN n-UV LED ( $\lambda_{\text{EL}} = 383$  nm) at different levels of current injection (at room temperature) along with pictures of the generated white light, blue emitting polymer, and green, yellow and red emitting NCs, and the location of the corresponding operating point on the  $(x, y)$  coordinates.

moving towards the planckian sources on the red side. Subsequently, the device is further hybridized with a 135 nm thick film of closely packed yellow NCs, yielding  $x = 0.32$ ,  $y = 0.37$ ,  $T_c = 5694$  K and  $R_a = 73.7$  (named CRI test sample 3). Here, the CRI further increases to 73.7 and the correlated color temperature further decreases to 5694 K. Finally, a 292 nm thick layer of closely packed red NCs is integrated on the very top. Consequently, this leads to an improved CRI of  $R_a = 83.0$  and a decreased correlated color temperature of  $T_c = 4052$  K at the operating point of  $x = 0.38$ ,  $y = 0.39$  (named CRI test sample 4). In figure 7, the EL spectra of sample 4 at different levels of current injection at room temperature are shown. A picture of the resulting white light and the location of the corresponding operating point on the  $(x, y)$  coordinates are also displayed. In figure 8, the evolution of the CRI from sample 1 to sample 4 is plotted, demonstrating a well-controlled CRI tuning and improvement from 49.5 to 83.0 by the controlled layer-by-layer assembly of polyfluorene and NC emitters. Such a high CRI satisfies the future lighting requirements of  $> 80$  CRI as road-mapped by Sandia National Laboratories [11], unlike the typical low CRI of yellow phosphor coated blue LEDs.

As a control group, alternative to the layer-by-layer integration, the blended mixture of NCs into the polymer is investigated. For this, the mixture contents of the NCs and the polyfluorene are carefully selected to obtain the highest feasible CRI while satisfying the white light condition. For this, 20  $\mu\text{l}$  blue polyfluorene ( $\lambda_{\text{PL}} = 439$  nm), 20  $\mu\text{l}$  green NCs ( $\lambda_{\text{PL}} = 540$  nm), 20  $\mu\text{l}$  yellow NCs ( $\lambda_{\text{PL}} = 580$  nm) and 10  $\mu\text{l}$  red NCs ( $\lambda_{\text{PL}} = 620$  nm) with concentrations of 3, 1.3, 1.3 and 2.2  $\text{mg ml}^{-1}$ , respectively, are blended. The n-UV LED ( $\lambda_{\text{EL}} = 383$  nm) is then hybridized with this blend of NCs in the polyfluorene host medium. The EL spectra of the resulting hybrid device at different levels of current injection at room

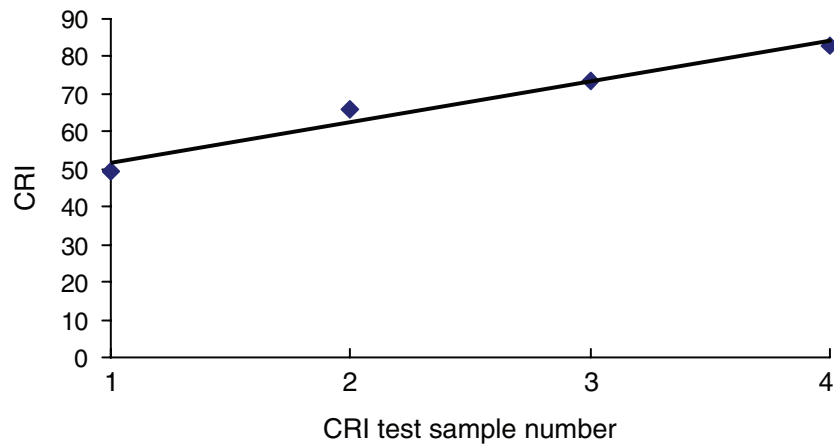


**Figure 8.** Controlling and improving CRI: CRI evolution from sample 1 to 4 by controlling the layer-by-layer assembly of polyfluorene and NC emitters.

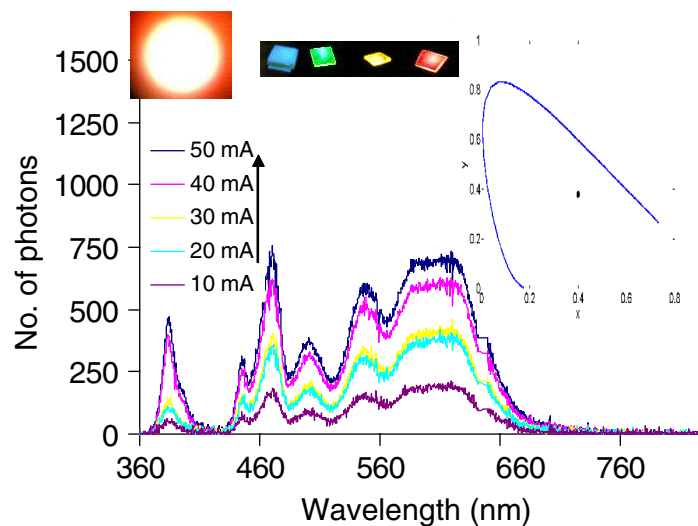


**Figure 9.** EL spectra of blends of yellow, green and red CdSe/ZnS core-shell NCs ( $\lambda_{PL} = 580, 540$  and  $620$  nm) in blue polyfluorene ( $\lambda_{PL} = 439$  nm) hybridized on a InGaN/GaN n-UV LED at different levels of current injection at room temperature along with pictures of the generated white light and emissions from blue conjugated polymer and green, yellow and red NCs, and the location of the corresponding operating point on the  $(x, y)$  coordinates.

temperature are given in figure 9. Additionally, a picture of the generated white light and the location of the corresponding operating point on the  $(x, y)$  coordinates is displayed in figure 9. This implementation experimentally leads to  $(x, y) = (0.40, 0.38)$ ,  $T_c = 3433$  K and  $R_a = 85.2$ , again falling within the white region of the CIE chromaticity diagram. In the case of blending, only a single film formation is required and the weighting factors of the contributing photoemission from the emitters in the film are controlled by the emitter concentration, as opposed to the layer-by-layer assembly, which requires multiple film formation and control of

**Table 2.** Hybrid polymer–NC WLED sample characteristics. (The last sample uses a blended mixture of NCs in polyfluorene, unlike the layer-by-layer assembly in the previous three samples.)

LED $\lambda_{\text{EL}}$ (nm)	Polymer $\lambda_{\text{PL}}$ (nm)	NC $\lambda_{\text{PL}}$ (nm)	( $x$ , $y$ )	$T_c$ (K)	$R_a$
383	439	580	(0.31, 0.27)	6962	53.4
383	439	540, 580	(0.23, 0.30)	14 395	65.7
383	439	540, 580, 620	(0.38, 0.39)	4052	83.0
383	439	540, 580, 620	(0.40, 0.38)	3433	85.2

the weighting factors of the emitters with each film thickness. As a result of the comparatively easier hybridization of such NC–polymer blends, a CRI that is slightly higher than the layer-by-layer deposition of the previous implementation is achieved. However, as also clearly seen in the picture of the generated white light from the NC–polymer blend, strong red emission comes off from the edges of the hybrid device due to reabsorption at short wavelengths and significant inhomogeneity of the emitters towards the edges in the blend. Consequently, in our implementation, the approach of layer-by-layer assembly of the NC and polyfluorene emitters is observed to be a better choice compared to the blending approach in terms of well-controlled light emission across the entirety of our hybrid device. In table 2, the hybrid WLEDs presented in this paper are summarized to list the EL peak wavelengths of the LEDs, the PL peak wavelengths of the NC and polymer emitters, the resulting ( $x$ ,  $y$ ) tristimulus coordinates, the correlated color temperature  $T_c$  and the CRI  $R_a$ .

In summary, the hybridization of our InGaN/GaN n-UV LEDs with different types of CdSe/ZnS core–shell NCs in combination with polyfluorene conjugated polymer was achieved to generate high-quality white light for the first time in different implementations as listed in table 2. The design, synthesis, growth, fabrication and characterization of these hybrid polymer-NC WLEDs were presented. With careful design and device implementation, such hybrid WLEDs were demonstrated to generate white light with high color rendering indices above 80, as is required for future solid-state lighting applications. Although the blended mixture of NC and polymer emitters also led to high CRI, strong red emission is observed coming off the edges of the hybrid device. With the dual use of conjugated polymers and NCs together on the same n-UV LED platform, the layer-by-layer hybridization was observed to achieve white light emission with high CRI, comparatively uniformly across the device when compared to the case of blending. Based on our proof-of-concept demonstration in this paper, we believe that such hybrid white light sources are promising for future lighting and display applications due to their highly tunable optical properties and high light quality.

## Acknowledgments

This work is supported by EU-PHOREMOST Network of Excellence 511616 within the 6th European Community Framework Program. Other support also includes a Marie Curie European Reintegration Grant MOON 021391 and TUBITAK EEEAG projects under nos 106E020, 104E114, 105E065 and 105E066 at Bilkent University. HVD acknowledges

additional support from the Turkish National Academy of Sciences Distinguished Young Scientist Award and SN and ES from TUBITAK Graduate Fellowship Program. Also, Professor Ullrich Scherf and Professor Ekmel Ozbay are kindly acknowledged for their support.

## References

- [1] Hirosaki N, Xie R, Kimoto K, Sekiguchi T, Yamamoto Y, Suehiro T and Mitomo M 2005 *Appl. Phys. Lett.* **86** 211905
- [2] Peon R, Doluweera G, Platonova I, Irvine-Halliday D and Irvine-Halliday G 2005 *Proc. SPIE* **5941** 109–23
- [3] Light Up the World Foundation online at <http://www.lutw.org>
- [4] US Department of Energy 2006 *LED Application Series: Recessed Downlights*
- [5] Lewotsky K 2006 *SPIE Professional* July 12–3
- [6] Landau S and Erion J 2007 *Nat. Photonics* **1** 31
- [7] Schubert E 2006 *Light-Emitting Diodes* (Cambridge: Cambridge University Press)
- [8] Yamada M, Narukawa Y, Tamaki H, Murazaki Y and Mukai T 2005 *IEICE Trans. Electron.* **E88–C** 9 1860
- [9] Chen H, Yeh D, Lu C, Huang C, Shiao W, Huang J, Yang C C, Liu I and Su W 2006 *IEEE Photonics Technol. Lett.* **18** 1430
- [10] Heliotis G, Gu E, Griffin C, Jeon C W, Stavrinou P N, Dawson M D and Bradley D D C 2006 *J. Opt. A: Pure Appl. Opt.* **8** 445
- [11] Tsao J Y 2004 *IEEE Circuits Devices* **20** 3
- [12] Cheon K E and Shinar J 2002 *Appl. Phys. Lett.* **81** 1738
- [13] Chuen C H and Tao Y T 2002 *Appl. Phys. Lett.* **81** 4499
- [14] D'Andrade B 2007 *Nat. Photonics* **1** 33
- [15] Paik K L, Baek N S, Kim H K, Lee J-H and Lee Y 2002 *Macromolecules* **35** 6782
- [16] Cheng G, Li F, Duan Y, Feng J, Liu S, Qiu S, Lin D, Ma Y and Lee S T 2003 *Appl. Phys. Lett.* **82** 4224
- [17] D'Andrade B W, Thompson M E and Forrest S R 2002 *Adv. Mater.* **14** 147
- [18] Chen S-A, Chuang K-R, Chao C-I and Lee H-T 1996 *Synth. Met.* **82** 207
- [19] Tasch S, List E J W, Ekström O, Graupner W, Leising G, Schlichting P, Rohr U, Geerts Y, Scherf U and Müllen K 1997 *Appl. Phys. Lett.* **71** 2883
- [20] Steuber F, Staudigel J, Stössel M, Simmerer J, Winnacker A, Spreitzer H, Weissörtel F and Salbecki J 2000 *Adv. Mater.* **12** 130
- [21] Lee Y-Z, Chen X, Chen M-C and Chen S-A 2001 *Appl. Phys. Lett.* **79** 308
- [22] Deshpande R S, Bulovic V and Forrest S R 1999 *Appl. Phys. Lett.* **75** 888
- [23] Nizamoglu S, Ozel T, Sari E and Demir H V 2007 *Nanotechnology* **18** 065709
- [24] Nizamoglu S, Ozel T, Sari E and Demir H V 2006 *IEEE COMMAD Conference on Optoelectronic and Microelectronic Materials and Devices (Perth, Australia)* WO-A5
- [25] Chen H, Yeh D, Lu C, Huang C, Shiao W, Huang J, Yang C C, Liu I and Su W 2006 *IEEE Photonics Technol. Lett.* **18** 1430
- [26] Chen H, Hsu C and Hong H 2006 *IEEE Photonics Technol. Lett.* **18** 193
- [27] Ali M, Chattopadhyay S, Nag A, Kumar A, Sapra S, Chakraborty S and Sarma D D 2007 *Nanotechnology* **18** 075401
- [28] Nizamoglu S and Demir H V 2007 *Nanotechnology* **18** 405702
- [29] Nizamoglu S and Demir H V 2007 *J. Opt. A: Pure Appl. Opt.* **9** S419
- [30] List E J W, Tasch S, Hochfilzer C, Leising G, Schlichting P, Rohr U, Geerts Y, Scherf U and Müllen K 1998 *Opt. Mater.* **9** 183
- [31] List E J W, Leising G, Schulte N, Schluer D A, Scherf U and Graupner W 2000 *Japan. J. Appl. Phys.* **2** **39** L760
- [32] Neher D 2001 *Macromol. Rapid Commun.* **22** 1365
- [33] Zhang C and Heeger A 1998 *J. Appl. Phys.* **84** 3

- [34] Talapin D V, Rogach A L, Kornowski A, Haase M and Weller H 2001 *Nano Lett.* **1** 207–11
- [35] Mutlugun E, Soganci I M and Demir H V 2007 *Opt. Express* **15** 1129
- [36] Sari E, Nizamoglu S, Ozel T and Demir H V 2007 *Appl. Phys. Lett.* **90** 011101
- [37] Demir H V, Sabnis V A, Fidaner O, Harris J S, Miller D A B and Zheng J F 2005 *IEEE J. Sel. Top. Quantum Electron.* **11** 86
- [38] Demir H V, Sabnis V A, Zheng J F, Fidaner O, Harris J S and Miller D A B 2004 *IEEE Photonics Technol. Lett.* **16** 2305–7
- [39] Sabnis V A, Demir H V, Fidaner O, Harris J S, Miller D A B, Zheng J F, Li N, Wu T C, Chen H T and Houngh Y M 2004 *Appl. Phys. Lett.* **84** 469–71